BNL-211926-2019-JAAM

Scaling Ability of the Counter-Current Flow Limitation (CCFL) Correlations for Application to Reactor Thermal Hydraulics

H. Glaeser, U. S. Rohatgi

To be published in "Nuclear Engineering and Design"

July 2019

Nonproliferation and National Security Department

Brookhaven National Laboratory

U.S. Department of Energy

USDOE National Nuclear Security Administration (NNSA), Office of Nonproliferation and Verification Research and Development (NA-22)

DISCLAIMER

Scaling Ability of the Counter-Current Flow Limitation (CCFL) Correlations for Application to Reactor Thermal Hydraulics

Horst Glaeser [1] and Upendra Singh Rohatgi [2*]

[1] Consultant, Germany; hglaeser@t-online.de
[2] Brookhaven National Laboratory, USA; rohatgi@bnl.gov
* Tel.: +01-631-344-2475

Abstract:

The limitation of gas-liquid counter-current flow is important for getting coolant to the core preventing heat-up. To illustrate the scaling dependence of counter-current flow in the downcomer, the upper core tie plate and the hot leg, some results are presented. Based on a derivation of the counter-current flow equations for vertical and horizontal flows, the scaling ability of existing correlations is shown for homogeneous vertical counter-current flow (Kutateladze-type equation) and separated horizontal flow in the hot leg during reflux-condenser conditions (Wallis equation). The large reactor scale heterogeneous counter-current flow in the downcomer and at the upper core tie-plate needed an extension of the Kutateladze-type equation. Bankoff suggested that for CCFL in perforated plates such as upper tie plate, a parameter that is a combination of actual length scale (Wallis parameter) and Laplace constant (Kutateladze parameter) will be required.

Keywords: Vertical homogeneous counter-current flow, vertical heterogeneous counter-current flow, horizontal separated counter-current flow, core bypass, emergency core cooling, scaling effects.

---

1. Introduction

Counter-current flow of gas and liquid appears in many places in a reactor system during phases of various transients. In most cases the liquid flows down and gas flows up, and they interact at the interface. The interaction at the interface that increases with gas flow rate opposes the liquid down-flow. Counter-current flow limitation (CCFL) is the limit of this liquid flow due to opposing gas flow. It has safety implication in getting coolant to the core and preventing heat-up in a Loss of Coolant Accident (LOCA).

There have been many experimental investigations at different scales to address CCFL. They are in pipes, annuli and plates with holes. The results were used to develop CCFL correlations. Two main correlations are known using the Kutateladze numbers or the Wallis numbers for steam and water momentum terms or non-dimensional phase velocities. The correlations can be derived from balance equations, see Glaeser (1992). Constants are used to adapt for specific geometries, wall effects, and deviations from assumptions, what is described in this chapter.

2. Correlations for the description of the counter-current flow limitation phenomenon

The CCFL is highly dependent on the geometry, orientation and configuration. In the following sections CCFL correlations for different configurations will be addressed.

2.1 Vertical counter-current flow

The steam-water counter-current flow is always coupled with instabilities of the gas - liquid interface. These instabilities may restrict the downwards liquid flow. The amplitude of a wave δ_l in Figure 1 can be evaluated as a function of the pressure difference between the crest of the wave and the base, assuming that the wave has a semispherical three-dimensional shape. It is assumed that the pressure difference between the bottom of the wave and the crest, i.e. the pressure difference perpendicular to the main flow directions, is equal to the dynamic head of the gas and liquid flows plus the gravity head of the wave. For the wave to be stable this pressure difference Δp needs to be balanced by surface tension σ. Thus, one gets the equation:

$$\boldsymbol{p_0 - p = \left(\rho_g^{1/2} v_g + \rho_l^{1/2} v_l\right)^2 - (\rho_l - \rho_g) g \delta_l \leq 2\sigma/\delta_l} \quad (1)$$

where v_g is the upwards gas velocity and v_l is the downwards liquid velocity and ρ is the density . This equation can be written as

$$\boldsymbol{\left(\rho_g^{1/2} v_g + \rho_l^{1/2} v_l\right)^2 / (\rho_l - \rho_g) g \delta_l \leq 2\sigma / \left[(\rho_l - \rho_g) g \delta_l^2\right] + 1} \quad (2)$$

For vertical counter-current flow the right-hand side of equation (2) decreases with increasing wave amplitude. The wave amplitude, however, is restricted due to the instability of the wave in vertical flow. A critical wavelength λ (Laplace coefficient) must be exceeded by the wave to become unstable (Taylor instability):

$$\boldsymbol{\lambda = \left[\sigma / \left(g(\rho_l - \rho_g)\right)\right]^{1/2}} \quad (3)$$

The steam up-flow disintegrate the unstable growing waves. Droplets, waves and liquid films may be carried upwards with the gas flow, limiting the water down-flow. For example, at a pressure of 400 kPa the critical wavelength of water in steam has a value of λ = 2.4 mm.

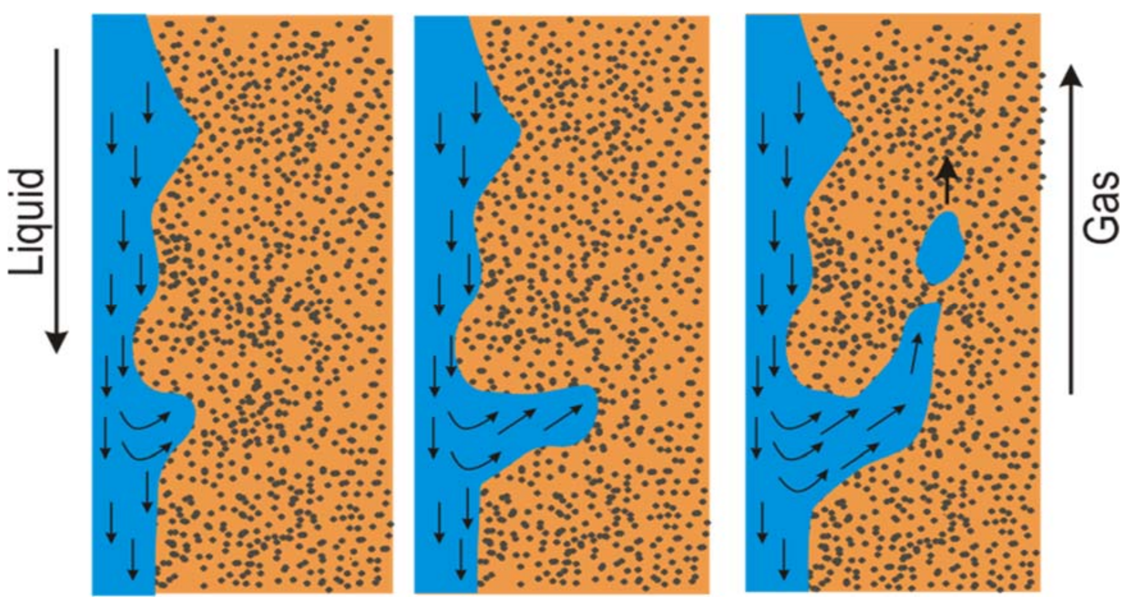

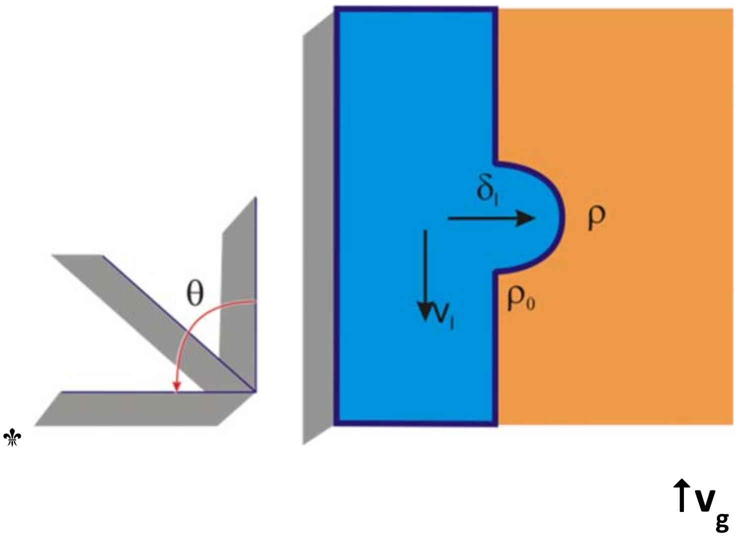

Figure 1. Waviness of the gas/ liquid interface and the effect of steam up-flow rate on water down-flow rate (Glaeser, 1992).

Defining a maximum wave amplitude

$\delta_l = \lambda/2$ (4)

for which the surface tension force can stabilize a wave of semi-spherical shape and introducing volumetric vapor fraction α and

superficial gas velocity $j_g = \alpha\, v_g$ (5)

superficial liquid velocity $j_l = (1-\alpha)\, v_l$ (6)

leads to the equation:

$$\rho_g^{1/2} j_g / \left\{\alpha\left[\sigma g\left(\rho_l-\rho_g\right)\right]^{1/4}\right\} + \rho_l^{1/2} j_l / \left\{\alpha\left[\sigma g\left(\rho_l-\rho_g\right)\right]^{1/4}\right\} \le (4+0.5)^{1/2} \quad (7)$$

One obtains the limiting value of j_g by maximizing j_l with respect to α, i.e. calculating the envelope as α is varied (Wallis, 1969). This eliminates the vapor fraction α, and the following relation is obtained:

$$\left\{\rho_g^{1/2} j_g / \left[\sigma g\left(\rho_l-\rho_g\right)\right]^{1/4}\right\}^{1/2} + \left\{\rho_l^{1/2} j_l / \left[\sigma g\left(\rho_l-\rho_g\right)\right]^{1/4}\right\}^{1/2} \le (4.5)^{1/4} \quad (8)$$

This equation is consistent with the empirical K-correlation using the Kutateladze numbers

$$K_g^{1/2} + m K_l^{1/2} = C \quad (9)$$

Where K is the Kutateladze number (Pushkina and Sorokin, 1969)

$$K_x = \rho_x^{1/2} j_x / \left[\sigma g\left(\rho_l-\rho_g\right)\right]^{1/4} \qquad x = g \text{ for gas or } l \text{ for liquid} \quad (10)$$

The constants in the empirical correlations are determined by experiments. According to equation (8) the constant C can be theoretically derived:

$C = 1.46.$ (11)

Pushkina and Sorokin (1969) found that C = 1.79 when $K_l = 0$ (onset of penetration). The Kutateladze number contains only physical properties and the superficial gas velocity for onset of penetration regardless of the size of the flow channel.

Some measured values for upper core tie plate and downcomer counter-current flow are:

- Tie plate: Karlstein 1/14 scale experiments (Simon et al., 1985): m = 0.77, C = 1.80.
- Tie plate: UPTF 1/1 scale entrainment/ de-entrainment experiments: m = 0.77, C = 1.64.
- Downcomer annulus: CREARE 1/5 scale experiments (Crowley et al., 1981): m = 0.82, C = 1.80.
- Downcomer annulus UPTF 1/1 scale needs an extension of the Kutateladze correlation and is described in section "*Vertical heterogeneous counter-current steam-water flow in the downcomer*".

The deviations of constant C between theoretical (C = 1.46) and measured values may be due to wall effects in small scale facilities, simplified assumptions and measurement errors in two-phase flow. Many more differently scaled experimental programs have been performed to address CCFL (Levy, 1999, Chapter 5). They are in pipes and annuli. Wallis and Kutateladze used tests in pipes of different sizes and liquid injection methods to develop CCFL correlations. The Wallis correlation is based on pipe diameter as length scale, see next section. However, this correlation diverges from data for larger diameter pipes. For pipes with larger diameters than 50 mm, the CCFL of steam and water can be represented by the Kutateladze correlation based on critical wave length and surface tension as described before. As discussed in the next section, the Wallis-type correlation is better suited for horizontal flow. The reason why the Wallis correlation fits the non-dimensional momentum fluxes of gas and liquid for small vertical scale is due to the relatively small flow cross section of sub-scale experimental facilities where the liquid film and the formation of waves is restricted by the diameter of the pipe or the gap width and circumference of an annulus.

The value of constant C for the Upper Plenum Test Facility (UPTF) experiments is closest to the derived theoretical value. The UPTF values in reactor scale were obtained from entrainment/ de-entrainment tests where water was injected via core simulator spray nozzles that distributed water droplets uniformly over the flow cross section, Figure 2. The water mass flow rate falling into the lower plenum was determined dependent on core simulator steam and water injection flow rates. In the case of homogeneous vertical steam-water counter-current flow, the Kutateladze-type correlation according to equations (8) and (9) is also valid for reactor scale geometries. However, this correlation was not found to be applicable in the case of asymmetric heterogeneous counter-current flow caused by Emergency Core Cooling (ECC) water injection via the cold or hot legs and the steam-water mixture flow out of the broken cold or hot leg. Based on these results it was necessary to develop a new correlation for heterogeneous counter-current flow in large-scale facilities (Glaeser, 1992).

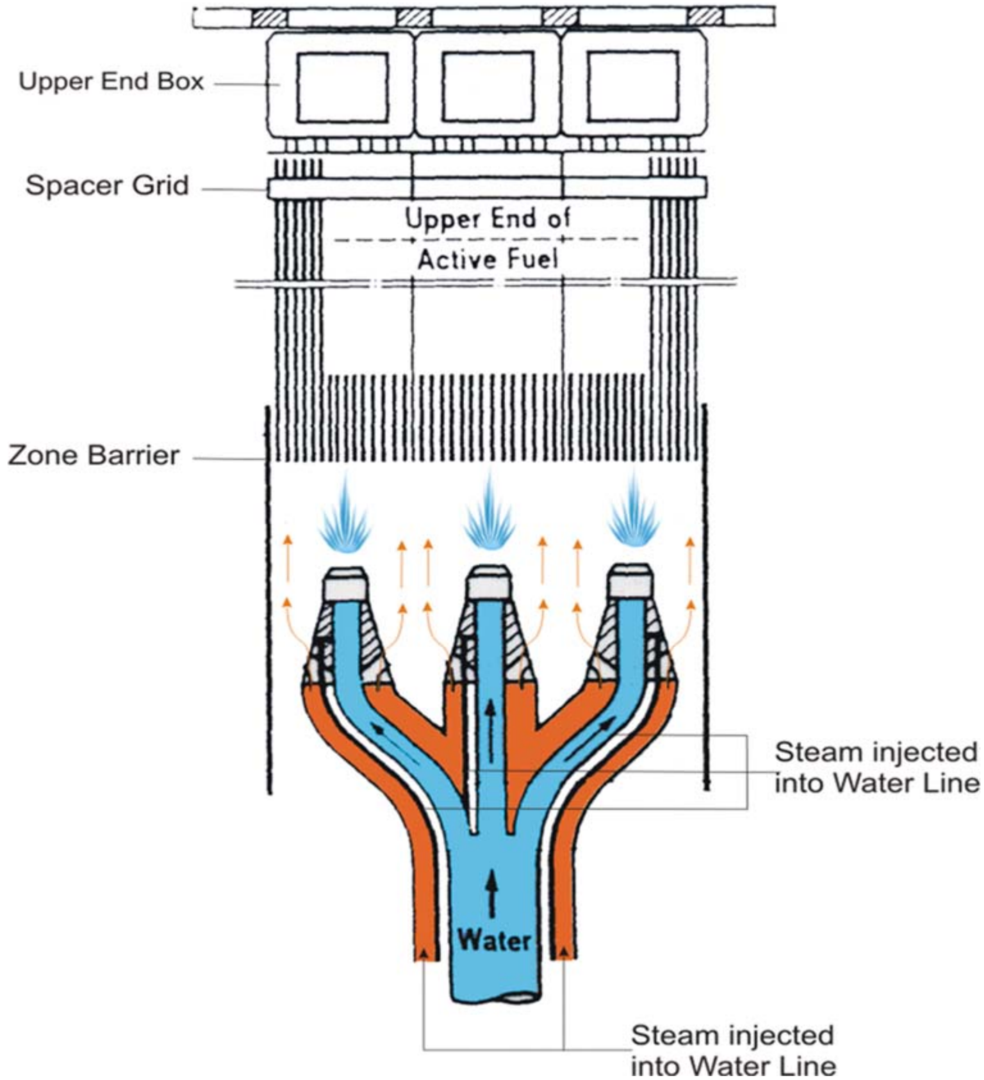

Figure 2. UPTF injection assembly of core simulator.p

2.2 Horizontal counter-current flow

In horizontal separated gas-liquid counter-current flow, the wave amplitude is not restricted by the critical wavelength, equation (3). The gravity head of the wave is directed perpendicular to the main flow direction in horizontal or inclined flow. The pressure difference Δp between the bottom of a wave and the crest due to the dynamic head of the gas and liquid flows in equation (1) needs to be balanced now by the gravity head of the wave and droplets acting perpendicular to the main flow directions of steam and water:

$$\boldsymbol{p_0 - p = \left(\rho_g^{1/2} v_g + \rho_l^{1/2} v_l\right)^2 = (\rho_l - \rho_g) g \delta_l} \quad (12)$$

We replace the wave amplitude δ_l in equation (12) by the diameter d of the flow channel:

$$\boldsymbol{\left(\rho_g^{1/2} v_g + \rho_l^{1/2} v_l\right)^2 / [(\rho_l - \rho_g) g d] = 1.0} \quad (13)$$

Introducing the superficial phase velocities j_x, equations (5) and (6), and calculating the envelope as the vapor fraction is varied we get

$$\left\{\rho_g^{1/2} j_g / \left[gd\left(\rho_l - \rho_g\right)\right]^{1/2}\right\}^2 + \left\{\rho_l^{1/2} j_l / \left[gd\left(\rho_l - \rho_g\right)\right]^{1/2}\right\}^2 = 1.0 \tag{14}$$

Equation (14) turns into the known empirical Wallis correlation:

$$j_g^{*1/2} + j_l^{*1/2} = C \tag{15}$$

where

$$j_x^* = \rho_x^{1/2} j_x / \left[gd\left(\rho_l - \rho_g\right)\right]^{1/2} \quad \text{x = g for gas or l for liquid.} \tag{16}$$

The constants in equation (16) are m = 1 and C = 0.7 – 1.0, depending on geometry and method of water injection (Wallis, 1969). The theoretical value from equation (14) is C = 1.0.

The Wallis correlation can be applied for counter-current flow characterized by unstable waves in horizontal oriented pipes of different scales from small to large size. This was demonstrated by a UPTF counter-current flow experiment investigating reactor scale hot leg reflux condenser conditions (Mayinger et al., 1992, Glaeser and Karwat, 1993, 2D/3D Program Work Summary Report, 1992, Reactor Safety Issues Resolved by the 2D/3D Program, 1993). Heat is transferred from the core to the secondary side of the steam generators by evaporation of water in the core and subsequent condensation of the steam in the U-tubes of the steam generators in the reflux condenser mode of a small break LOCA. A portion of the condensate flows back from the steam generator to the upper plenum counter-currently to the steam through the hot leg. That condensate serves cooling the core. Due to momentum exchange between the steam-flow and the water-flow in the hot legs counter-current flow limitation may occur, which could prevent or at least deteriorate the water flow back to the core cooling the fuel rods.

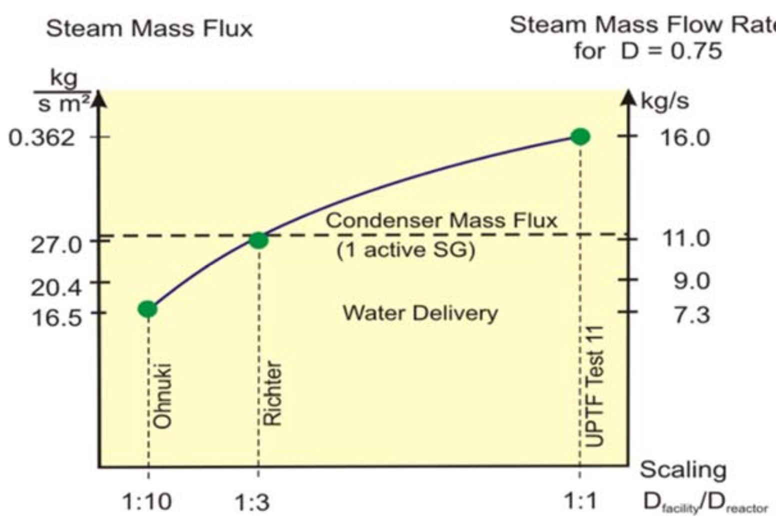

Figure 3. Water delivery limit to upper plenum compared with reactor steam mass flow towards steam-generator in the hot leg (Glaeser and Karwat, 1993).

The UPTF test has demonstrated that a substantial margin exists between the CCFL and the typical conditions expected in a Pressurized Water Reactor (PWR) during reflux condenser mode of a small break LOCA. This is the case for water delivery limit to the upper plenum in a full reactor scale hot leg of 750 mm diameter, see Figure 3 (Glaeser and Karwat, 1993). The steam mass flow results from a 2% core decay power scaled from 8 MPa to 0.3 MPa pressure of UPTF.

The location of counter-current flow limitation for reflux condenser mode is obviously in the inclined part of the hot leg to the steam generator inlet (angle to the horizontal axis = 50°). The constants in the Wallis equation (15) from the UPTF hot leg experiment are (2D/3D Program Work Summary Report, 1992, Figure 4.8-6) m = 0.85 and C = 0.69, see Figure 4.

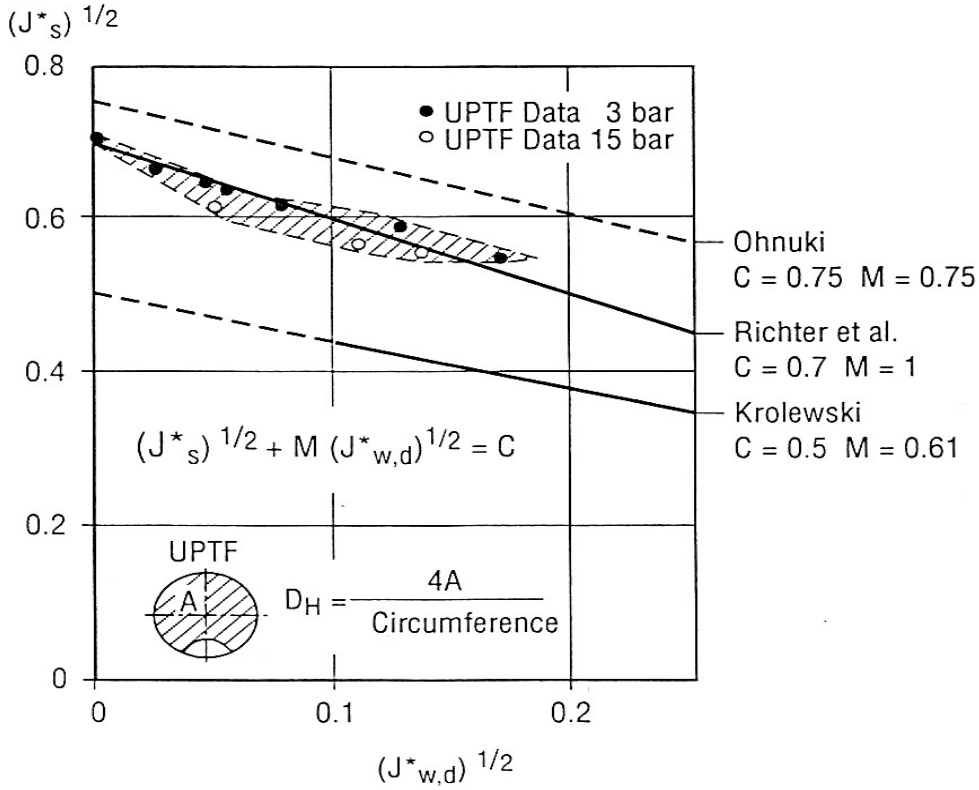

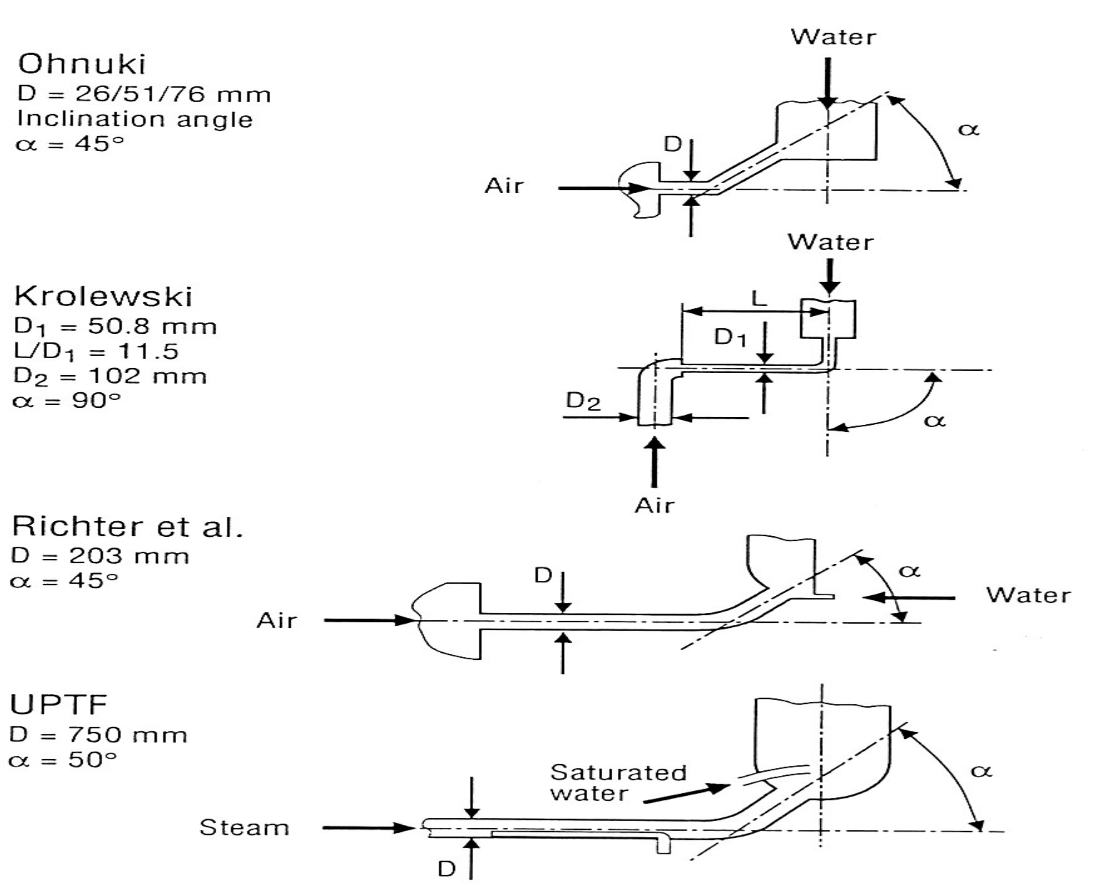

Figure 4. Comparison of UPTF counter-current flow data in hot leg with correlations of small-scale experiments (2D/3D Program Work Summary Report, 1992, Figure 4.8-7).

Al Issa and Macian (2011) issued an extensive review of experimental work performed on CCFL in the hot leg of a PWR. The experiments showed different geometries, length to diameter ratios, different inclinations of the riser to the horizontal part, bend shapes and inlet geometries. Only a few experimental facilities represent the full-scale hot leg of a PWR. The authors compared a high number of experiments under the different effects, like water velocity, geometrical effects, physical properties, hysteresis, condensation effects, shear stress, pressure drop and void fraction. Counter-current flow is caused by droplet entrainment, slugging and large roll-waves.

Deendarlianto, Höhne, Lucas and Vierow (2012) present another comprehensive review of research work on counter-current gas–liquid two-phase flow in a PWR hot leg, and provide direction regarding future research on this topic. In order to clarify some contradictions of experimental results, one should look to the geometrical parameters, the sub-scale dimensions of the experimental facilities and distinguish between vertical, inclined and horizontal countercurrent flow in the pipes. The available analytical work is grouped into three categories: (1) one-dimensional stratified two-fluid model, (2) semi-analytical investigations, and (3) scaling parameters. One important point of their publication is the application of computational Fluid Dynamics Codes (CFD) to calculate CCFL in a hot leg during reflux condenser conditions. A considerable robust three-dimensional closure relation for this application is not yet achieved due to lack of detailed phenomenological knowledge and due to application of empirical one-dimensional experimental correlations to the multidimensional flows. They used a gas/liquid inhomogeneous multiphase flow model coupled with a shear stress transport (SST) turbulence model. A new concept of shear stress coefficient in the algebraic interfacial area density model (AIAD) was used. The results indicated that quantitative agreement of the CCFL characteristics between the calculation and experimental data was obtained as shown in Figure 5. Information on subcooling of the steam-water experiment and calculation is not given in the paper. The difficulty mentioned by the authors is that the important parameters on CCFL cannot be measured, like interfacial shear. This may be one of the reasons for limited success in mechanistic modelling of flooding. The authors claim that advanced measurements, such as the optimized optical technique and recently developed mesh wire sensor are needed in the near future. Mesh wire sensor can be used to provide the information of the cross sectional distribution of the steam volume fraction. It is necessary to recognize detailed structures of flows during CCFL.

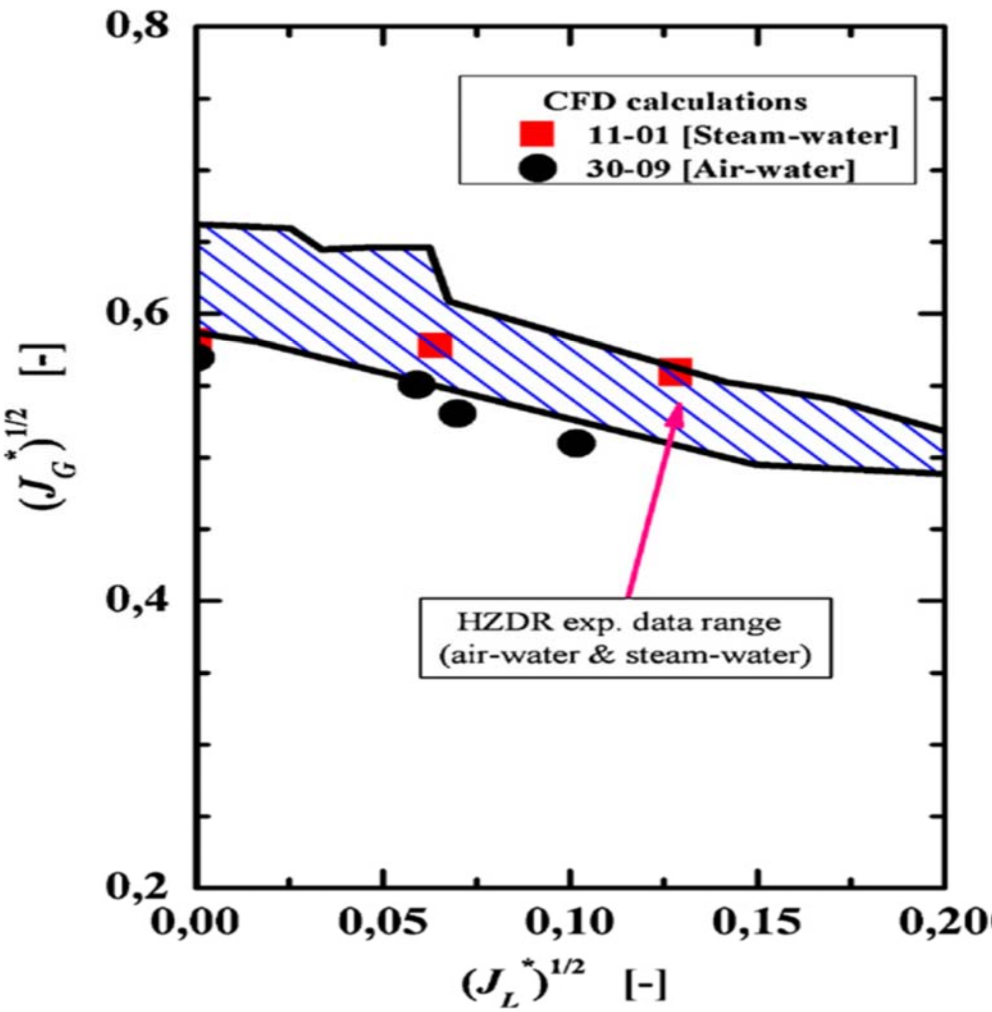

Figure 5. Calculated CCFL characteristics in a model of PWR hot leg (Deendarlianto et al., 2012).

2.3 Vertical heterogeneous counter-current steam-water flow in the downcomer

To illustrate the scaling dependence of heterogeneous vertical steam-water counter-current flow in the downcomer, some results are presented. That phenomenon is important for efficient core cooling by the ECC systems during a loss of coolant accident when a large break of a main coolant pipe occurs. Before UPTF experiments were performed, insight of downcomer phenomena during cold leg ECC-injection had been developed particularly based on the USNRC ECC Bypass Program. It contained steam-water tests, which were performed at 1/30, 1/15, 2/15 and 1/5 length scale at the Battelle Columbus Laboratories and at CREARE. Steady state CCFL tests with steam up-flow and ECC-water down-flow as well as transient tests involving lower plenum flashing and two-phase up-flow were carried out. Table 1 summarizes the dimension of different scale downcomer tests.

Table 1. Scale of different test facilities.

	PWR	UPTF		CREARE (1/5)		BCL (2/15)		CREARE (1/15)		CREARE (1/30)	
		Actual	Scale*	Actual	Scale	Actual	Scale	Actual	Scale	Actual	Scale
Vessel Diam	4.4 m	4.87	1.1	0.89 m	0.2	0.618 m	0.14	0.292 m	0.066	0.152 m	0.034
DC, Gap●	0.26 m	0.25 m	0.96	0.038 m	0.146	0.031 m	0.119	0.0126 m	0.048	0.0064 m	0.025
DC, Height	5.33 m	6.64 m	1.25	1.37 m	0.257	0.82 m	0.153	0.46 m	0.086	0.229 m	0.043
LP, Depth●	1.94 m	2.48 m	1.28	1.52 m	0.783	1.022 m	0.526	0.86 m	0.443	0.528 m	0.272
LP Vol, M^3	29.6	24.9	0.84	0.94	0.032	0.302	0.010	0.058	0.0019	0.0096	3×10^{-4}
Cold Leg Diam	0.74 m	0.75 m	1.01	0.152 m	0.21	0.21	0.102 m	0.0476 m	0.064	0.076 m	0.1
$D_{CL/D}$	0.168	0.154	—	0.168	—	—	0.165	0.163	—		0.5

*Scale is the ratio of actual dimension to PWR dimension
●Lower plena are deeper and gaps are narrower in subscaled facilities

Empirical CCFL correlations based on experimental data of these down-scaled test facilities have been developed, using two dimensionless phase velocities, a modified Wallis parameter containing "W" as an average downcomer annulus circumference, and the already mentioned Kutateladze number.

$$j_x = \frac{\dot{M}_x}{\rho_x A_{DC}} \frac{\rho_x^{1/2}}{[gW(\rho_w - \rho_s)]^{1/2}} \tag{17}$$

$$K_x = \frac{\dot{M}_x}{\rho_x A_{DC}} \frac{\rho_x^{1/2}}{[g\sigma(\rho_w - \rho_s)]^{1/2}} \tag{18}$$

In spite of the variation of scale of the test facilities between 1/30 and 1/5, the extrapolation to full scale downcomer geometry was not clear until experiments on UPTF were performed.

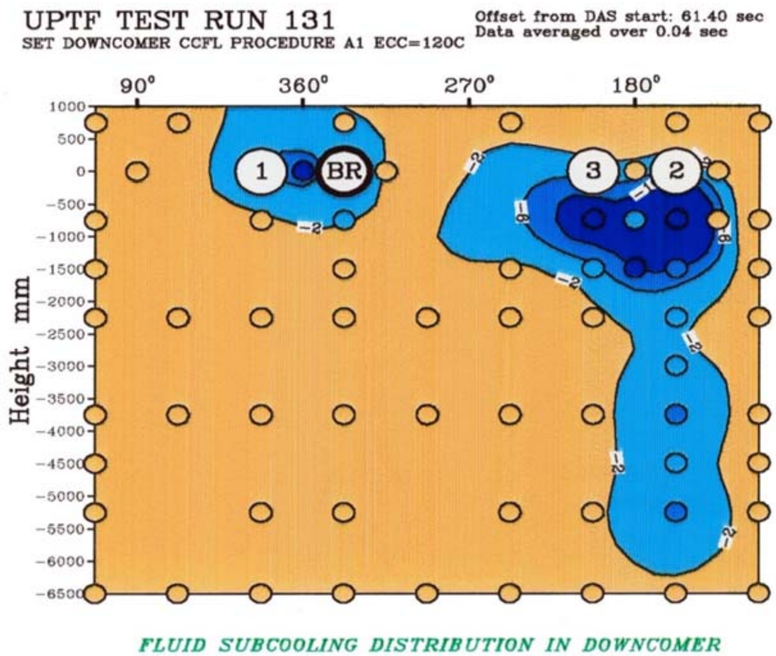

Figure 6. Heterogeneous counter-current flow conditions in full-scale downcomer for subcooled ECC water, distribution of subcooled temperatures.

To provide CCFL and ECC core by-pass data for full reactor geometry, tests on UPTF were carried out. The result of a UPTF experiment, simulating the downcomer behavior during the end-of-blowdown and the refill phases for a large cold leg break is shown in Figure 6. The test was carried out at a reactor typical steam up-flow of 320 kg/s and ECC-water injection (subcooling 115 K) into the three intact cold legs of the four loops. The contour plot shows isotherms of fluid temperatures (subcooling) in the downcomer projected in a plane. The two-dimensional presentation shows strongly heterogeneous steam-water flow conditions which were not observed in small-scale experiments. The ECC-water delivered from the cold legs 2 and 3, which are located opposite to the broken loop connection, penetrates the downcomer without being strongly affected by the up-flowing steam. Most of the ECC-water delivered from cold leg 1, which is located close to the broken cold leg, however, flows directly to the break bypassing the core.

To demonstrate the effect of the facility scaling on downcomer CCFL, the data obtained from CREARE, BCL and UPTF were compared (Beckner and Reyes, 1981, Rohatgi, 1993, Boyack et. al., 1989). Beckner and Reyes (1981) developed correlations for each facility accounting for condensation. These correlations represented data and were plotted in Wallis and Kutateladze space (Rohatgi, 1993). There are three possible flow configurations in downcomer. In narrow downcomers the liquid will form bridges and globules and interact with the gas. There will be larger interfacial area density. Wallis type correlation will be more suitable. The second possibility is for bigger downcomer where liquid flows in form of film. The interaction is at the film interface and countercurrent flow leads to instability and increased roughness due to wave amplitude. The Kutateladze type of correlations will be more suitable. The third possibility is for very large downcomers such as UPTF or plant where liquid films falls under the cold legs and gas flows to the break. The interaction at the interface is weak. For smaller facilities the flow configurations could be a combination of first two types. The smallest facility (CREARE 1/30) exhibits different behavior and could be due bridging and break up. It does not follow same behavior as other bigger facilities. An example of plot of correlation in Wallis space is shown in Figure 7 and in Kutateladze space in Figure 8. In general, the critical superficial gas flow for complete bypass is lower for smaller facilities as expected. It is clear the assumption of interaction of liquid film and air is very different for UPTF and ECCS injection under two cold legs flows towards lower plenum. It will require a different flooding curve as discussed later. Figure 6 shows the liquid down flow configuration in UPTF.

UPTF and CREARE with 1/5 scaling are compared in references (Glaeser, 1992, Glaeser and Karwat, 1993, 2D/3D Program Work Summary Report, 1992, Glaeser and Wolfert, 2012). Slightly subcooled ECC water was used in this UPTF test and saturated ECC water on CREARE. Due to the strongly heterogeneous flow conditions in the full-scale downcomer of UPTF the water delivery curve of UPTF is significantly higher than for CREARE.

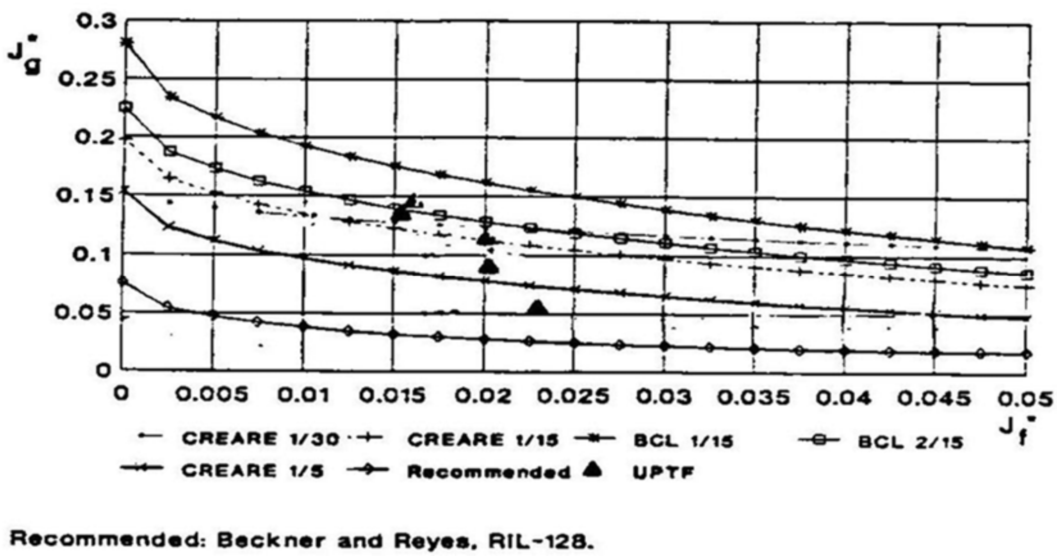

Figure 7. Flooding curves for different scale facilities in Wallis space.

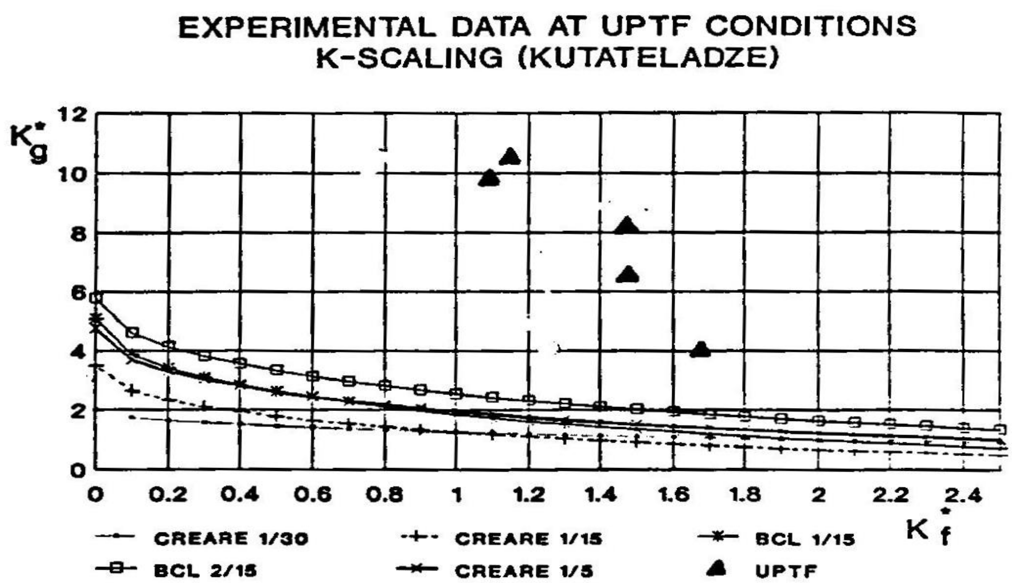

Figure 8. Data plotted in Kutateladze space for different facilities.

The main findings with respect to downcomer behavior during the end-of-blowdown and refill phases of a large cold leg break with cold leg or downcomer ECC-injection can be summarized as follows:

- A significant scale effect on downcomer behavior can be observed,
- Steam-water flow conditions in the downcomer are highly heterogeneous at full scale,
- Heterogeneous or multi-dimensional behavior increases water delivery rates at full-scale relative to previous tests on down-scaled facilities,
- CCFL correlations developed from the down-scaled tests are not applicable to full-scale downcomer,
- Downcomer CCFL correlations for cold leg ECC injection based on down-scaled test results under-predict the water penetration to the lower plenum at full scale,
- Due to strong heterogeneous flows in a real downcomer, a CCFL correlation must account for the location of the ECC injection relative to the broken cold leg.

To describe the vertical asymmetric heterogeneous gas-liquid counter-current flow in the full scale downcomer, the Kutateladze type flooding equation was extended by Glaeser (1992) correlating the local steam velocities of the multi-dimensional flow field with the superficial steam velocity. A geometrical lateral distance between the legs with ECC injection and the broken loop is introduced in the gas up-flow momentum term. This term relates the local upward gas velocity at the water down-flow locations to the superficial gas velocities. The superficial gas velocity can be calculated from the steam mass flow rate. The CCFL-correlation for the downcomer is then with ν_g kinematic gas viscosity and g gravitational acceleration:

$$\boldsymbol{K_g^{1/2}\left(\frac{\nu_g^{2/3}}{g^{1/3}L}\right)^{1/2} + 0.011K_l^{1/2} = 0.0245} \tag{19}$$

with the geometric length

$$\mathbf{L = 0.5\,\pi\, d_{outer}\, sin^2(0.5\theta_{ECC\text{-}BCL})} \tag{19a}$$

The correlation is applicable for

$$\boldsymbol{\frac{g^{1/3}L}{\nu_g^{2/3}} \geq 5400} \tag{20}$$

If there is more than one ECC injection location, the arithmetic mean value of all distances L between the ECC injection legs and the broken leg has to be used in the correlation. However, only those injection locations can be considered where water can flow downwards. This means that the modified non-dimensional gas velocity obtained by using the value of L for the individual injection location has to be below the onset of penetration point. Otherwise, the respective ECC injection leg cannot be included in the arithmetic mean value L. More details of the derivation and application of the Glaeser-correlation can be found in Glaeser(1992) and Glaeser and Karwat (1993).

Figure 9 shows the modified gas up-flow expression versus the liquid Kutateladze number. The curve according to equation (19) gives a good representation of all data points obtained with saturated water injection, and for subcooled water reducing the steam up-flow superficial velocity by the condensation rate (Glaeser and Karwat, 1993). Water down-flow is not possible above the curve.

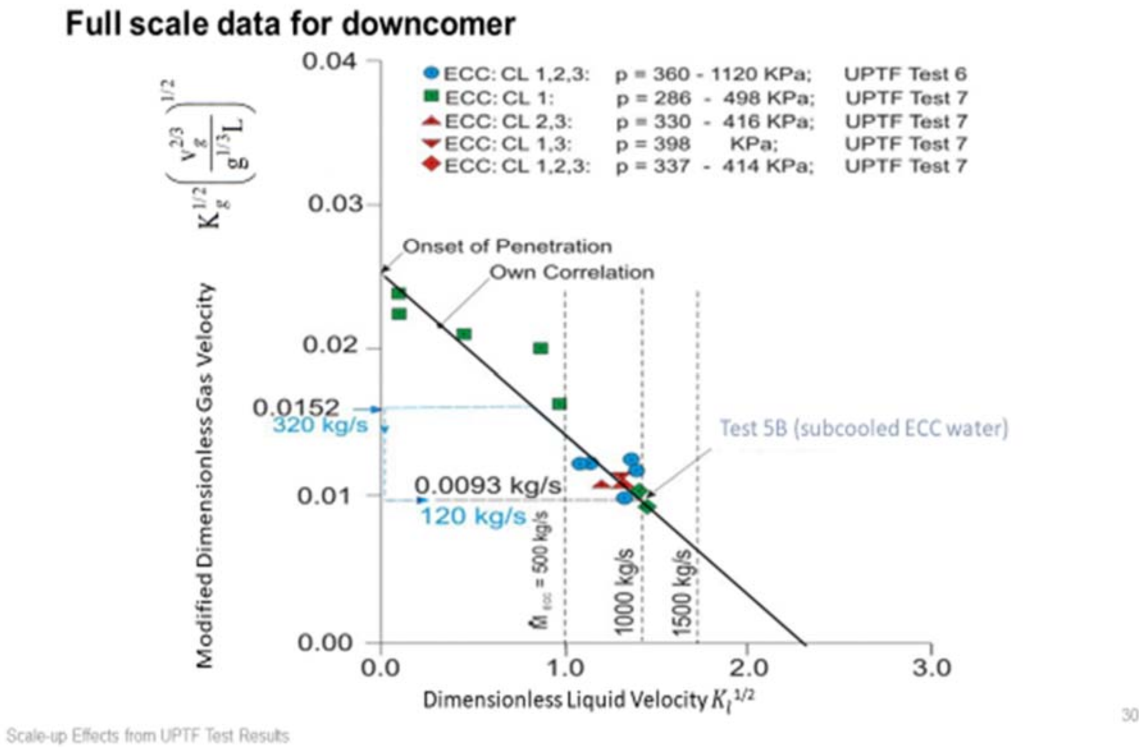

Figure 9. CCFL correlation for heterogeneous steam-water flow derived from downcomer data on UFTF (Glaeser, 1992, Glaeser and Karwat, 1993).

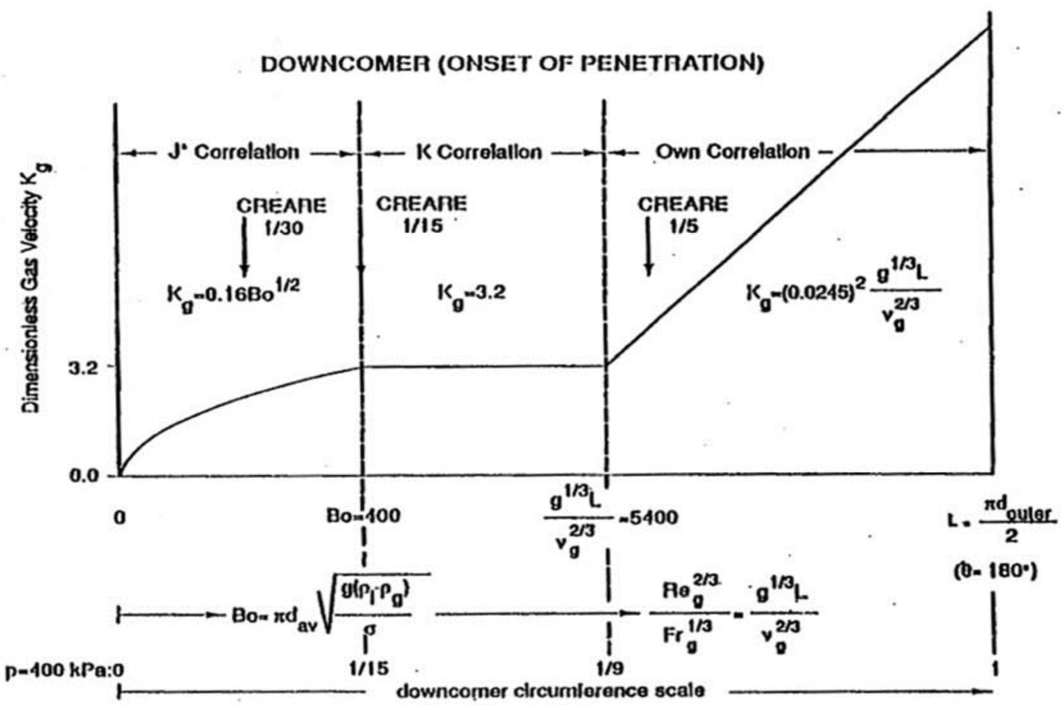

Figure 10. Downcomer CCFL correlation for zero penetration of liquid (total core bypass) (Glaeser, 1992).

The resulting lowest gas velocity for zero water penetration (onset of penetration) is shown in Figure 10 compared with the downcomer circumference scale. Water down-flow is impossible for gas velocities above the curve. Three different CCFL correlations are applicable for three different scaling regions. These are the classical Wallis- and Kutateladze-type as well as the Glaeser-correlation. The range of applicability is dependent on the dimensionless annulus circumference, which governs the different flooding correlations. It can be seen that it is impossible to extrapolate counter-current flow correlations from small-scale data below one-ninth downcomer circumference scale (equivalent to 1/81 flow cross section scale) to reactor scale. The full-scale UPTF data were needed to clarify the influence of scaling on the CCFL phenomenon.

2.4 Vertical heterogeneous counter-current steam-water flow through the upper tie-plate

ECC water injected into the hot legs via a special Hutze nozzle at the bottom of the hot legs (KWU reactor design) or water coming from the steam generators and pressurizer is flowing into the upper plenum and from there through the upper core tie plate as the narrowest flow cross section into the core region. The other possibility is that the water flows with the steam flow out of the broken hot leg. Counter-current flow tests through the upper tie plate were performed with saturated water concerning the tie plate. The main interest, however, was in the reactor-typical subcooled ECC water injection tests. An asymmetric, heterogeneous water downflow and steam or steam-entrained water up-flow region was observed in the upper plenum and tie plate region like in the downcomer, Figure 11. Thus, the description of counter-current flow in the large-scale tie plate region is similar to the large-scale downcomer, for both the saturated and subcooled ECC water tests. The counter-current flow correlation with the constants determined from saturated ECC water tests on UPTF is:

$$\boldsymbol{K_g^{1/2}\left(\nu_g^{2/3}/\left(g^{1/3}L\right)\right)^{1/2}+0.014K_l^{1/2}=0.027} \qquad (21)$$

with the geometric length

$$L = d_e \sin(0.5\ \theta_{ECC\text{-}BHL}) \qquad (22)$$

where the equivalent diameter d_e of the tie plate flow cross section is

$$d_e = (4A_{TP} / \pi)^{1/2}. \qquad (23)$$

A_{TP} is the total tie plate flow cross section.

The correlation is applicable for

$$4400 \le g^{1/3}\ L / \nu_g^{2/3}. \qquad (24)$$

If there is more than one ECC injection location, the arithmetic mean value of all distances L between the ECC injection legs and broken leg has to be used in equation (21). Only those injection locations are to be considered where water can flow downward. The modified non-dimensional gas velocity obtained by using the value of L for the individual injection location has to be below the onset of penetration point. For low values of the geometric length L, equation (21) turns into the Kutateladze type equation (9). The experimental results in Figure 11 can be represented by one curve using equation (21) (Glaeser, 1992).

UPTF tests were also performed with subcooled ECC water, and with steam-water up-flow through the tie plate simulating water entrainment from the core region increasing the upward momentum. The steam and steam-water mass flow rate were not high enough to prevent an ECC water down-flow through the tie-plate. When subcooled water passes the tie plate downward, a part of up-flowing steam condenses below the tie plate reducing the upward steam mass flow.

The higher ECC water down-flow through the tie plate and in the downcomer in reactor size compared with small-scale experimental results and the effect of steam condensation leads to a lower relevance of CCFL as a safety issue regarding core cooling.

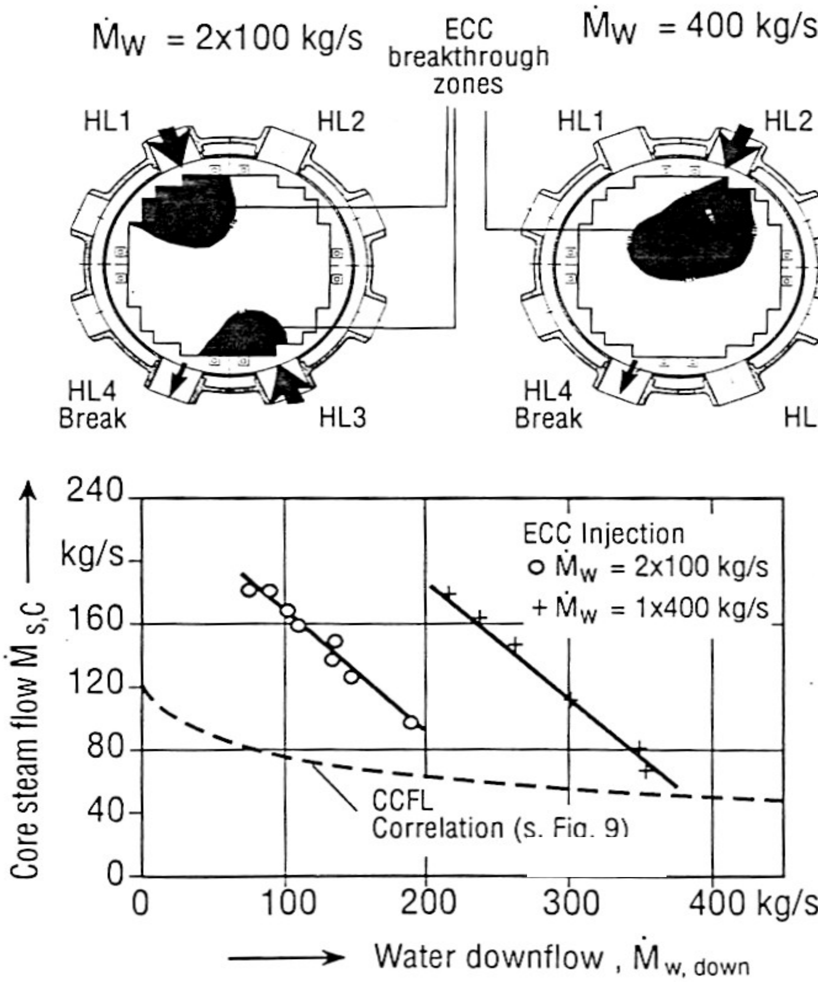

Figure 11. Upper tie-plate flow distribution for water injection into hot legs 1 and 3 or into hot leg 2, and experimental results compared with Kutateladze type equation (9), taken from 2D/3D Program Work Summary Report, 1992 (section 4.4.3).

2.5 Vertical sub-scale counter-current flow through the upper tie plate

Tests for BWR upper tie plate were performed to develop CCFL correlations (No et. Al., 2005, Bankoff et. al, 1981). Bankoff (1981) did tests with different configurations of holes in the horizontal plate as shown in Figure 12.

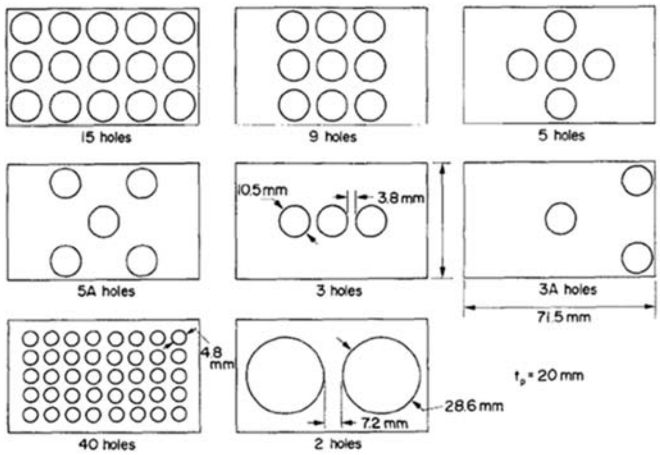

Figure 12. Arrangements of holes in horizontal plate in Bankoff's Test (Bankoff et. al. 1981)

Bankoff showed that Wallis and Kutateladze type of correlations did not represent the data as shown in Figures 13 and 14.

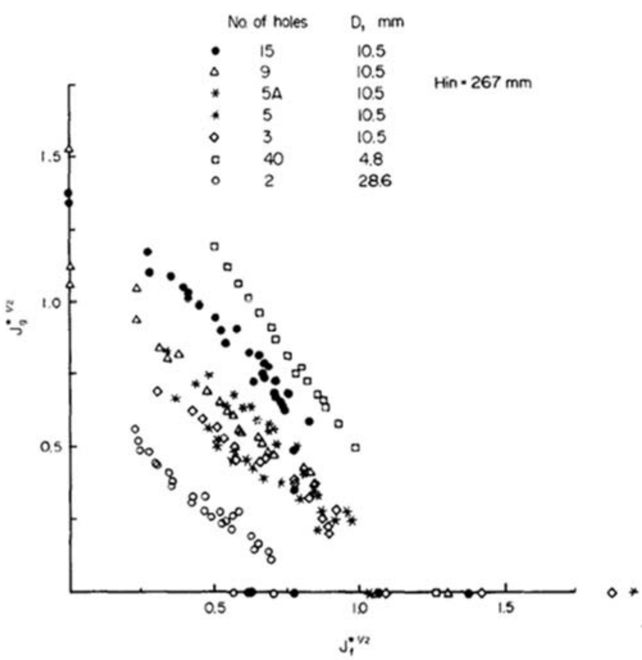

Figure 13. Bankoff's data plotted in Wallis parameter space (Bankoff et. al. 1981)

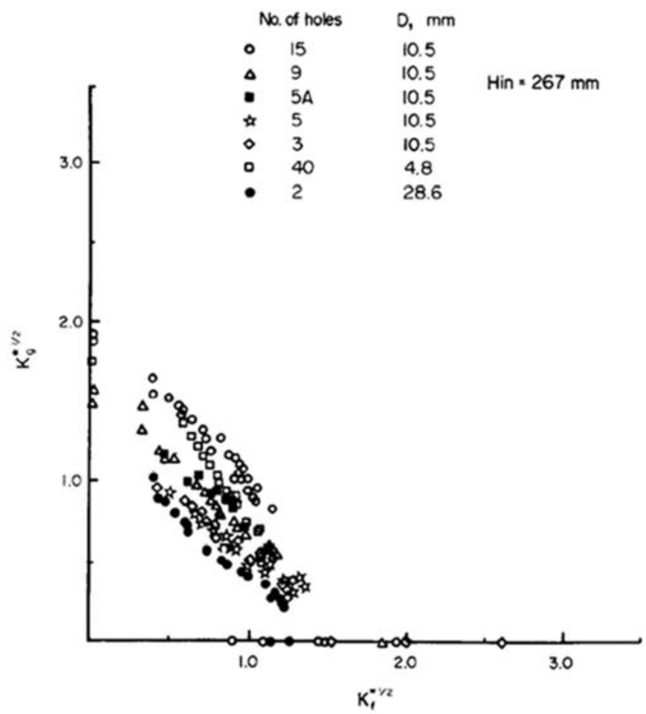

Figure 14. Bankoff's data plotted in Kutateladze space (Bankoff et. al. 1981)

Bankoff proposed another similar correlation based on the length scale as function of whole diameter and Laplace capillarity constant.

$$\boldsymbol{H_k^* = j_k \left[\frac{\rho_k}{gw(\rho_f-\rho_g)}\right]^{1/2}} \tag{25}$$

Where length scale w is an interpolated quantity between length scales used in Wallis correlation and Kutateladze correlation as defined here

$$\boldsymbol{w = d^{1-\beta}L_1^{\beta} \qquad 0 \leq \beta \leq 1} \tag{26}$$

And, Laplace constant is given as,

$$\boldsymbol{L_1 = \left[\frac{\sigma}{g(\rho_f-\varrho_g)}\right]^{1/2}} \tag{27}$$

The interpolating parameter, β, is a function of plate geometry,

$$\boldsymbol{\beta = tanh(\gamma k_c d)} \tag{28}$$

And

$$\boldsymbol{\gamma = \frac{nA_h}{A_p}} \tag{29}$$

$$\boldsymbol{k_c = \frac{2\pi}{t_p}} \tag{30}$$

Bankoff's correlation is as follows;

$$H_g^{*\,1/2} + H_f^{*\,1/2} = C \qquad \textbf{(30)}$$

And,

$$C = 1.07 + 4.33 * 10^{-3} L^{*} \qquad L^{*} < 200 \qquad \textbf{(31)}$$

$$C = 2 \qquad L^{*} > 200 \qquad \textbf{(32)}$$

The Bond number, L*, is given as follows for n holes

$$L^{*} = n\pi d \left[\frac{g(\rho_f - \rho_g)}{\sigma}\right]^{1/2} \qquad (33)$$

Bankoff's data is plotted in Bankoff's parameter space as shown in Figure 15. The data converge in a straight line.

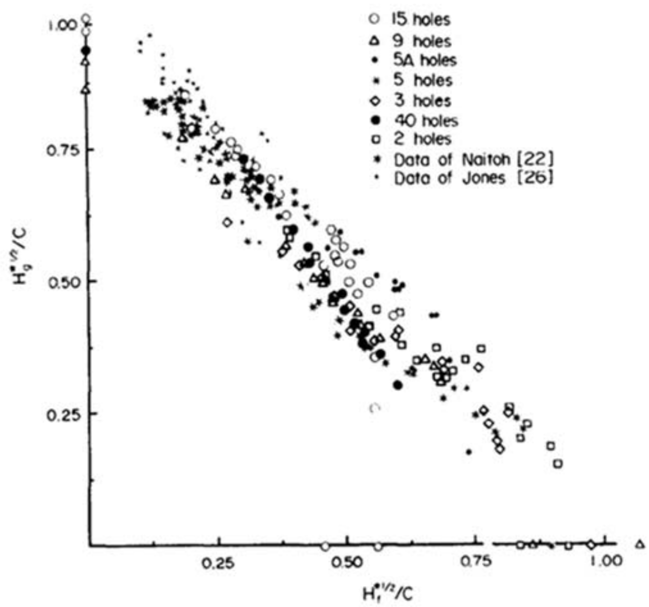

Figure 15. Bankoff's data plotted in Bankoff's parameter space (Bankoff et. al. 1981)

After Bankoff' s correlation, another experiment was conducted for plate with 4 holes with diameter of 5 cm (No et.al., 2005) as shown in Figure 16. The hole sizes are bigger than the biggest hole size in Bankoff's test.

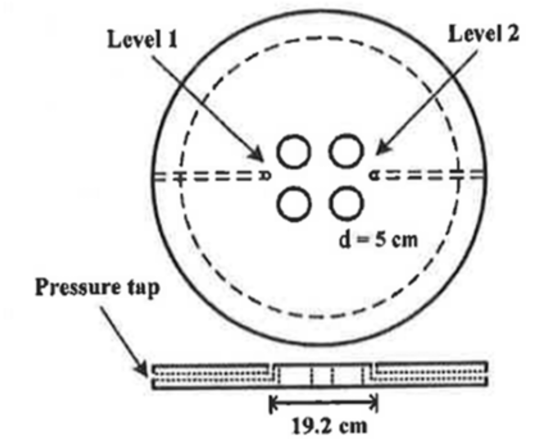

Figure 16. Hole distribution in circular plate in test, (No et. al . 2005)

No et. al. (2005) have shown that Bankoff's correlation does not match data for hole diameter greater than 2.86 cm as shown in Figure 17.

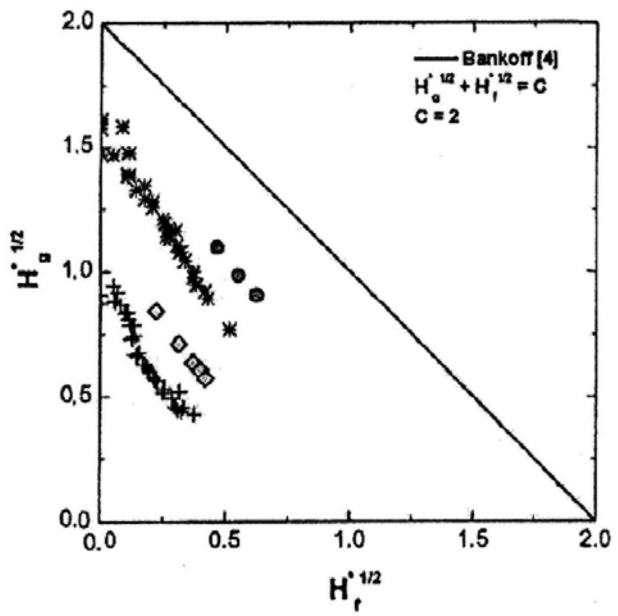

	dh (cm)	t (cm)	n	dp (cm)	Reference
•	5	1	4	9.6	No[2005]
◊	5	4	4	9.6	No[2005]
Ж	3.6	7.2	3	11.6	Zhang[1992]
+	3.6	72	3	11.6	Zhang[1992]

Figure 17. Comparison of No's and Zhang's data with Bankoff's correlation (No et. al. 2005)

No et. al. (2005) proposed an alternate correlation for larger holes. The correlation is as follows.

$$j_g^{*\,1/2} + 1.22 j_f^{*\,1/2} = 0.88 \quad for\ d \geq 2.86\ cm \tag{34}$$

This correlation is compared with data in Figure 18 and match is better than Bankoff's correlation.

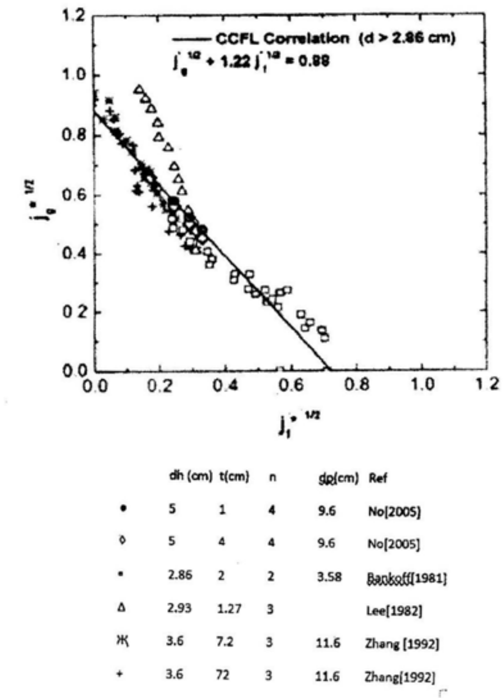

Figure 18. No et al.(2005) correlation for larger holes

Sobajima, (1981) conducted spray cooling tests in ROSA-III facility and also addressed CCFL phenomena at upper tie plate. The hole sizes 1-2 cm. There tests were performed at high pressures, 6 bar to 31 bars. His CCFL data fell below Bankoff's correlation. Sobajima concluded that this is due to high pressure conditions in his test and Bankoff test was a low pressure.

3. Conclusions

Counter-current flow limitation has been observed in different locations in the reactor system such as PWR downcomer, perforated upper tie plate and hot leg flows. The phenomena are due to the interaction of liquid and gas flowing in counter current direction and instability at the interface. Different correlations apply for vertical homogeneous or small-scale countercurrent flow and heterogeneous large scale counter-current flow. The downcomer flow tests indicated that small scale tests prevented down flow at lower gas flow rates due to strong interaction between liquid film and gas flow. However, full scale UPTF indicated that flow phenomena were very different from sub- scale facilities with much less interaction and CCFL correlations developed from sub-scale experiments do not apply. A different CCFL correlation is proposed.

Similarly, for perforated plates countercurrent correlation phenomena are different for different scales and heterogeneous vertical countercurrent flows. Earlier investigations for sub-scale experiments use the length scale interpolated between hole size and Laplace constant. This correlation works up to a size but for larger hole sizes a correlation similar to Wallis was proposed. A different CCFL correlation for heterogeneous reactor scale counter-current flow through the upper core tie plate of a PWR is proposed, based on Kutateladze numbers considering critical wave length and surface tension.

In horizontal oriented pipes of different scales from small to large size, the Wallis correlation can be applied for counter-current flow over the whole scaling range. This was demonstrated by small scale experiments and a UPTF counter-current flow experiment investigating reactor scale hot leg reflux condenser conditions.

Correlations, like the presented CCFL-correlations are used as closure relations in thermal-hydraulic system computer codes. Such codes are important scaling tools to perform safety analysis for power reactors. Strong connections are there between scaling, code validation, setting up the nodalization and uncertainty evaluation as well as code user qualification and expertise. The refinement of the thermal-hydraulic system-codes and the completion of the validation for the simulation of full size plant accidents are important tasks. The scalability of CCFL correlations, thereby of the codes, requires that the flow regime or flow configurations remain the same in the facilities of interest.

Another important effort in the analytical work will be focused on the development of two-phase flow CFD-codes. Due to the high resolution in space and the possibility for three-dimensional description of the single- and two-phase flow phenomena, the scaling issue may become less important. Parallel to the progress in the development of the computer hardware with respect to calculation time the application area of these codes will be extended. The development of the two-phase flow CFD-codes is a great challenge for the analytical teams in the next decades and may contribute to the motivation of young scientists working in the field of nuclear technology. It is hoped that two phase CFD will be mature enough to predict CCFL for different geometries and orientations.

References

2D/3D Program Work Summary Report, 1992. Edited by Damerel, P.S., Simons, J.W., MPR Associates Inc., GRS-100, Garching, Germany.

Al Issa, S. Macian, R., 2011. A review of CCFL phenomenon. Annals of Nuclear Energy 38 (2011), 1795-1819.

Bankoff, S.G, Tankin, R.S., Yuen, M.C., and Hsieh, C.L.,1981. " Countercurrent Flow of Air/water and Steam/water Through a Horizontal Perforated Plate", Int. J. Heat and Mass Transfer, Vol 24, No. 8, pp. 1381-1395, 1981.

Beckner, W. and Reyes, J., 1981," Lower Plenum Refill Research Results", https://www.nrc.gov/docs/ML1725/ML17254A308.pdf

Boyack, B., Catton I., R.B. Duffey, R.B., Grifith, P., Katsma, K.R., Lellouche, G.S., Levy, S., Rohatgi, U.S., Wilson, G., Wulff , W. and Zuber, N., 1989. "Quantifying Reactor Safety Margins - Application of Code Scaling, Applicability and Uncertainty Evaluation Methodology to a Large Break, Loss-of-Coolant Accident," USNRC NUREG/CR-5249, December 1989.

Crowley, C.J., Rothe, P.H., Sam, R.G., 1981. 1/5-scale countercurrent flow data presentation and discussion. CREARE Inc., NUREG/CR-2106, November 1981.

Deendarlianto, Höhne, T., Lucas, D., Vierow, K., 2012. Gas–liquid countercurrent two-phase flow in a PWR hot leg: A comprehensive research review. Nuclear Engineering and Design, 243 (2012) 214-233.

Glaeser, H., 1992. Downcomer and tie plate countercurrent flow in the Upper Plenum Test Facility (UPTF). Nuclear Engineering and Design 133 (1992) 259-283.

Glaeser, H., Karwat, H., 1993. The contribution of UPTF experiments to resolve some scale-up uncertainties in countercurrent two-phase flow. Nuclear Engineering and Design 145 (1993) 63-84.

Glaeser, H., Wolfert, K., 2012. Scaling of thermal-hydraulic phenomena and system code assessment; Seminar on the Transfer of Competence, Knowledge and Experience Gained through CSNI Activities in the Field of Thermal-hydraulics, THICKET-3. OECD/NEA Headquarters, Issy-les-Moulineaux, France, 25-29 June 2012.

Lee, H.M., McCarthy, G.E., and Tien, C.L. 1982. ”Liquid Carryover and Entrainment in Air-Water Countercurrent Flooding”, EPRI report NP-2344, 1982

Levy, S., 1999. Two-Phase Flow in Complex Systems. John Wiley & Sons, New York.

Mayinger, F., Weiss, P., Wolfert, K., 1992. Two-phase flow phenomena in full-scale reactor geometry; CSNI Specialist Meeting on Transient Two-Phase Flow, Aix-en-Provence, France, 6-8 April 1992.

No, H.C., Lee, K., and Song, C., 2005. “An Experimental Study on Air/water Countercurrent Flow limitation in Upper Plenum with Multi-Hole Plate”, Nuclear Engineering and Technology, Vol 37, No. 6, December 2005

Pushkina, O.L., Sorokin, Y.L., 1969. Breakdown of liquid film motion in vertical tubes, Heat Transfer-Soviet Research 1, No. 5 (1969) 56-64.

Reactor Safety Issues Resolved by the 2D/3D Program, 1993. Edited by Damerel, P.S., Simons, J.W., MPR Associates Inc., GRS-101, Garching, Germany.

Rohatgi, U.S. and Neymotin, L, (1993). ”Assessment of Scaling of Pressurized Water Reactor Emergency Core Coolant Bypass Flow Tests. In: Ashpis D.E., Gatski T.B., Hirsh R. (eds) Instabilities and Turbulence in Engineering Flows. Fluid Mechanics and Its Applications, vol 16. Springer, Dordrecht, 1993

Simon, U. et al., 1985. UPTF Calibration Tests, Abschlussbericht FE-Vorhaben BMFT 1500 664. KraftwerkUnion, Technischer Bericht R 54/85/14.

Sobajima, M., 1981. ” Spray Cooling Test, A Separate Effect Test and ROSA-III, A BWR-LOCA Simulation Facility”, Journal of Nuclear Science and Technology, 18(8), pp 629-639, August, 1981

Wallis, G.B., 1969. One-Dimensional Two-Phase Flow. Mc-Graw-Hill.

Yamamoto, Y., Akiba, M., Morooka, S., Shirakawa, K. and Abe, N., 2006. ” Thermal Hydraulic Performance of Tight lattice Bundle”, JSME International Journal, series B., Vol 49, No. 2, 2006

Zhang,J., Seynhaeve, J.M.,and Giot,M. 1992. ”Experiments on the Hydrodynamics of Air-Water Countercurrent Flow through Vertical Short Multitube Geometries”, Experimental Thermal and Fluid Science, 5, pp 499-514, 1992